

## ***Letter to the Editor of the ACP Manuscript “An estimation of the $^{18}\text{O}/^{16}\text{O}$ ratio of UT/LMS ozone based on artefact CO in air sampled during CARIBIC flights” by S. Gromov and C. A. M. Brenninkmeijer***

S. Gromov (on behalf of all authors)

Correspondence to: S. Gromov ([sergey.gromov@mpic.de](mailto:sergey.gromov@mpic.de))

Dear Dr. Kaiser,

We are very grateful for your great attention to this work and constructive comments that helped us to improve the quality of this manuscript significantly. Following your suggestions, we have prepared the revised version (please, find the pages with mark-up at the end of this letter). We have addressed all your comments (shown below italicised), on a few of them we have a different opinion, as we discuss in the following.

We appreciate very much the time you spent for editing this paper.

With kind regards,

Sergey Gromov

*The manuscript appears fragmented due to the number of appendices and supplementary materials. I think the appendices can stay as they are (but see my comments below regarding their contents). However, please merge Figs. S2, S3 and S4 with the main text. Fig. S1 could stay in the supplementary information, but since this would just leave one figure in the supplementary information, you might want to merge it with the main text at an appropriate location as well.*

We have merged the figures (including Fig. S1) from the supplement material with the main text of the revised manuscript.

*My main concerns the so-called "contamination kinetic framework" in Appendix A. The term is misleading because it implies some sort of kinetic modelling, which has no taken place. Instead, you appear to have some sort of regression analysis, but is unclear what was regressed against what and you might want to add a figure to illustrate this.*

We disagree here with the understanding of the Editor that “framework” implies modelling. According to Oxford Dictionary, the definition of “framework” (<http://www.oxforddictionaries.com/definition/english/framework>) is:

*1.1 A basic structure underlying a system, concept, or text.*

It is the structure or concept of what chemistry we conjecture might have happened in the CARIBIC-1 inlet/tubing that produced artificial CO with the oxygen signature of that of  $\text{O}_3$ . We also disagree that a “some sort of regression analysis” was done; it is necessary to understand which variables one needs to regress against which in order to obtain sensible information. We cannot put a set of concrete chemical equations because we do not know which (and how many) reactions have occurred. (That is why, by the way, we use a conceptual notation, see below.) Nonetheless, we could establish a functional dependency between the contamination strength and some parameters, *e.g.*  $[\text{O}_3]$ . Understanding and quantifying such dependency is only possible applying certain concepts, *i.e.* within a framework. Ultimately, our task here is to communicate to the Reader how one can tackle a problem with so many unknowns.

We note that the figure illustrating the regression ( $C_c$  as a function of  $[\text{O}_3]$ ) is already included in the manuscript, see Fig.1 (d).

*The mathematical presentation is completely incomprehensible and the units on the left hand side and right hand side of the equation do not match. The notation using round brackets is not defined. What does ... stand for? What are "stoichiometric factors"? I have only heard of stoichiometric coefficients. Why do these "factors" appear as indices? What do you mean by integral stoichiometric factors? Maybe integer?*

Eq. (A1) (first line) is given in a conceptual way (we refer to our answer above) – that is why it does not resemble “normal” chemical equations. We believe, however, that it does not impede a chemist (a physicist, a scientist) to understand it, does it? As an ellipsis commonly denotes “omitted”, here, obviously standing in place of educts and products, it denotes some (unknown) educts and products. We could replace them with “R”s and “P”s, which will require additional explanation instead of current more intuitive way, and may even confuse the Reader, since some of “P”s may turn out to be “R”s in the next reaction. That is why it is difficult to use the conventional set of chemical equations here. Instead, we show the most important part – that X and O<sub>3</sub> have to react once or several times to produce CO. Further, why any “round brackets notation” has to be defined? Brackets are commonly used to separate a set of words, expressions, *etc.* Equations can also be separated. In our case, brackets separate equations according to the educt, *i.e.* we distinguish reactions of either O<sub>3</sub> or X, which are important for delivering oxygen and carbon to the final CO produced. The indices *K* and *κ* (which are explained below in this paragraph of the manuscript) denote how many reactions occur, *i.e.* how many times O<sub>3</sub> or X may have reacted in order to produce CO. As more than one reaction may happen before one CO molecule is produced, we have to account for the stoichiometry of this kinetic system. We, in contrast, have heard of “stoichiometric factors” (you may like to use the following link to get a notion on the amount of chemical literature using this term:

[https://www.google.de/search?tbm=bks&hl=en&q=%22stoichiometric+factor%22+&=&gws\\_rd=ssl](https://www.google.de/search?tbm=bks&hl=en&q=%22stoichiometric+factor%22+&=&gws_rd=ssl) ). Essentially, “factor” and “coefficient” are often used with the same meaning – they define the proportionality, here between the number of reacted and produced molecules. Because our formulation is more conceptual and not a strict chemical one, we chose using “stoichiometric factors”. (We admit that using “overall” suits here better than “integral” meaning, however, also the same.)

Furthermore, we ascertain that the units in Eq. (A1) (second line) *do match*:

$$C_c [\text{nmol/mol}] = \lambda_{\text{O}_3} \cdot k_c \tau_c \cdot [\text{O}_3]^2 = [\text{unitless}] \cdot [\text{mol/nmol}] \cdot [\text{nmol/mol}]^2 = [\text{nmol/mol}]$$

This formulation does not pertain to chemical kinetics, it relates the amount of artefact CO (in mole fraction units) to the abundance of O<sub>3</sub> (in mole fraction units) measured concomitantly and uses mole fraction units for the sake of convenience (see also our answer below on the comment to l. 83). We certainly agree that using it in the same equation line is misleading (see the amendments to that we propose below).

*What is the value of  $k_c$  you refer to.*

One cannot infer (or use in calculation) the value of  $k_c$  without knowing the reaction time  $\tau_c$  and yield  $\lambda_{\text{O}_3}$  (which are not known, too). Nevertheless, we essentially require only the product of  $k_c$ ,  $\lambda_{\text{O}_3}$  and  $\tau_c$  in order to estimate the contamination strength, and this value was derived and communicated in the manuscript (*i.e.*  $C_c/[\text{O}_3]^2$  of  $(5.19 \pm 0.12) \cdot 10^{-5}$  mol/nmol).

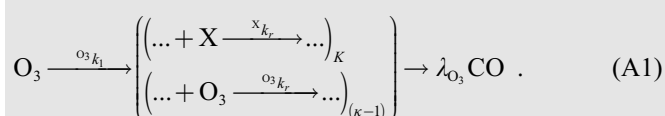
*I suggest you rewrite this "framework" as a set of a chemical equations (this can be examples or placeholders) and derive any purported mathematical relationship from the corresponding kinetic rate equations (where applicable).*

Due to reasoning outlined above, we are not able to formulate the framework in a strict system of chemical equations – at least in the way that will ease its understanding. As a consequence, we cannot derive any purported mathematical relationship, except of that general one shown in Equation (A1) (second line).

We agree, however, that the kinetic framework is poorly described and lacks clarity. To amend it, we split Eq. (A1) into three separate equations and add a more detailed description of the conceptual formulation we use (first line of Eq. (A1)) and of the ensuing mathematical relationships that were used in the regression. We propose the following amendment to the Appendix A:

## Appendix A. Contamination kinetic framework

We infer the functional dependence of the CO contamination strength in the kinetic framework conceptually formulated as follows:



Eq. (A1) reads that production of an artefact CO molecules is initiated by O<sub>3</sub> (via either its decomposition or a reaction with an unknown educt) and is followed by a set of unknown reactions which proceed via unknown educts or products (denoted with ellipses), however requiring at some step an incorporation of carbon (donated by carbonaceous species X) and

oxygen (also possible in secondary O<sub>3</sub> reactions) atoms into final CO. Coefficients  $K$  and  $\kappa$  describe the stoichiometry of the system, *i.e.* how many reactions of X and O<sub>3</sub> (with the individual unknown rate coefficients  $^Xk_r$  and  $^{O_3}k_r$ ) lead to production of one artefact CO, respectively. The yield  $\lambda_{O_3}$ , a diagnostic quantity, relates the amount of artefact CO molecules produced to the total number of O<sub>3</sub> molecules consumed in the system. Based on Eq. (A1), the functional dependence of the artefact CO component (denoted  $C_c$ , obtained by discriminating the C1 outliers from respective C2 data) on [O<sub>3</sub>] or [X] is generally formulated as (abundances in number density units are used)

$$C_c = \int_{\tau_c} \prod_{\kappa} ^{O_3}k_r [O_3] \prod_K ^Xk_r [X] dt, \quad (A2)$$

where  $\tau_c$  denotes the contamination reaction time. Eq. (A2) defines the regression expression using which we attempted to fit the values of  $C_c$  as a function of  $\kappa$ , [O<sub>3</sub>],  $K$  and [X] (the latter was chosen iteratively from a set of carbonaceous species measured). Practically, however, this regression analysis ascertains that variations in  $C_c$  are exhaustively described using [O<sub>3</sub>] and  $\kappa$ . Furthermore, we find that no other species or operational parameter (*e.g.* temperature, pressure, flight duration, latitude, *etc.*) measured in C1 appear to determine (correlate with)  $C_c$ . Based on this, we can reduce Eq. (A2) to its final, simpler form, *viz.*

$$C_c = \lambda_{O_3} k_c [O_3]^\kappa \tau_c, \quad (A3)$$

where  $k_c$  denotes the overall pseudo-first-order rate coefficient of the reaction chain that is exclusively propelled by O<sub>3</sub>. The product ( $\lambda_{O_3} k_c \tau_c$ ) thus integrates the influence of the unknown (and likely invariable) [X],  $^Xk_r$ ,  $K$  and  $\tau_c$ . Finally, regressing  $C_c$  using Eq. (A3) provides its best approximation as a function of [O<sub>3</sub>] at  $\kappa = 2.06 \pm 0.38$ , suggesting two chain steps involving O<sub>3</sub> or its derivatives. At  $\kappa = 2$ , the product ( $\lambda_{O_3} k_c \tau_c$ ) that proportionates the CO contamination strength and [O<sub>3</sub>] is found to be  $(5.19 \pm 0.12) \cdot 10^{-5}$  mol/nmol ( $\pm 1\sigma$ , *adj. R*<sup>2</sup> = 0.83, *red. χ*<sup>2</sup> = 4.0; mole fraction units are used here for convenience). The low uncertainty (within  $\pm 3\%$ ) of this estimate confirms an exclusive dependence of the contamination source on the O<sub>3</sub> abundance, as well as much similar reaction times  $\tau_c$ . The regressed value of  $C_c$  as a function of [O<sub>3</sub>] is presented in Fig. 1 (d) (solid line). It is possible to constrain the overall yield  $\lambda_{O_3}$  of CO molecules in the artefact source chain to be between 0.5 and 1, comparing the magnitude of  $C_c$  to the discrepancy between the [O<sub>3</sub>] measured in C1 and C2 ( $\pm 20$  nmol/mol, taken equal to the [O<sub>3</sub>] bin size owing to the N<sub>2</sub>O–O<sub>3</sub> and H<sub>2</sub>O–O<sub>3</sub> distributions matching well between the datasets). Lower  $\lambda_{O_3}$  values, otherwise, should have resulted in a noticeable (*i.e.*, greater than 20 nmol/mol) decrease in the C1 O<sub>3</sub> abundances with respect to the C2 levels.

*Consider replacing the ambiguous term "mixing ratio" with the clearer and - by intuition - more easily understandable "mole fraction".*

We would like to keep the term “mixing ratio”, because 1) It is widely used when measurements of trace gases like CO and O<sub>3</sub> are reported (also often in ACP), 2) We reduce the ambiguity by explicitly mentioning the tracer, *i.e.* “CO mixing ratio”, and 2) It will spare us from re-rendering several figures in the manuscript.

*Please spell out "w.r.t." - there is no need to abbreviate this.*

Spelled.

*Lines 62, 66, 67 87, 102, 154, 289: Please delete the tilde signs and where necessary give the actual uncertainties of the values.*

Done.

*65: Please define STP - 1 bar, 273.15 K? 1.01325 bar, 298.15 K?*

Done.

*71: The delta and R indices not clear. 13C, 18O and 17O are not suitable superscript indices because they lead to a double superscript index; please use delta(18O), R(18O), R\_st(18O) etc. instead.*

For ultimate clarity, we decided to refrain from using indices for R. Regarding the  $\delta$ -values, we keep the isotope mass number to identify them (*e.g.*, <sup>13</sup> $\delta_c$  and <sup>18</sup> $\delta_c$ ) to avoid double superscripting.

74: You might want to cite my re-evaluated  $^{13}\text{C}/^{12}\text{C}$  isotope ratio (Kaiser, *Geochimica et Cosmochimica Acta* 2008, doi:10.1016/j.gca.2007.12.011) ... I am not saying you should.

We would like to keep the current reference. We are aware that this value is nominally outdated since the last re-determination of the carbon isotope ratio of the NBS 19 used to define the “hypothetical” V-PDB scale. Owing to the differences between the former (*i.e.*, assigned from PDB) and revised scales, a change in isotope composition implies *ex post facto* different absolute abundances derived using the same  $\delta^{13}\text{C}$  values reported. The resulting  $\delta^{13}\text{C}$  signatures presented here are sensitive to the choice of the  $^{13}\text{C}/^{12}\text{C}$  standard ratio. Nonetheless, errors introduced by adopting outdated reference value are negligible compared to uncertainties introduced by the other factors, *e.g.* laboratory measurement or estimates with the MM. Using the re-evaluated  $^{13}\text{C}/^{12}\text{C}$  ratio would imply re-calculation and re-plotting of all data, which we would like spare ourselves from. Ultimately, the  $\delta^{13}\text{C}(\text{CO})$  values we report may be easily recalculated employing the re-evaluated (or any other)  $^{13}\text{C}/^{12}\text{C}$  standard ratio.

83: IUPAC has reserved square brackets are reserved for molar concentrations (units of  $\text{mol dm}^{-3}$ ). If you redefine their meaning, please avoid being ambiguous and use for either mole fraction or number density, not both. On p. 12, you use square brackets for number densities.

Although indeed in the kinetic calculations we used number densities ( $\text{molecules}/\text{cm}^3$ ), we presented the formulation in Appendix A using mole fraction units in order to facilitate reporting of the contamination magnitude (*e.g.*, in  $\text{nmol}/\text{mol}$ ). This is also seen in the  $C_c/[\text{O}_3]^2$  ratio reported in  $\text{mol}/\text{nmol}$  units.

85: "every 130 s"

Replaced.

88: Add comma after "viz."

Added.

93: Replace "ibid., Panel (b)" with "Figure 1 b".

Replaced.

98: "stratospheric influence increases"

We reformulate it as “With  $\text{O}_3$  rising,  $[\text{CO}]$  decreases to typical stratospheric values, ...”

110,195: Replace ; with .

Replaced.

119: Replace *ibid.*

Replaced.

145: use of subscript indices is not ideal because of length of index and space ("in situ")- use bracket index notation instead?: "Delta(WAS-in situ)"

We bracket index notation, thank you.

146: There should be brackets around ( $5.3 \pm 0.2$ ) to indicate that the unit "nmol/mol" applies to the value and its uncertainty.

Corrected.

146 & Fig. 3: Define SD (sometimes you use sigma; what's the difference?).

We change “SD” to “standard deviation”. Here we emphasise that the uncertainty quoted is the population standard deviation divided by the square root of the sample size. Below in this paragraph we also present the spread of  $\Delta(\text{WAS-in situ})$ , which is the standard deviation of the population only.

151: "situ" needs to be subscript;

Corrected similar to that for l. 145.

167, 183: There is no advantage of using rho; please stick with  $[\text{CO}]/[\text{O}_3]$ .

We have replaced  $\rho_{\text{O}_3:\text{CO}}$  with “ $[\text{O}_3]:[\text{CO}]$ ”.

201: stilted language - please replace "It therefore stands to reason to conclude" by "We therefore conclude", you also use active language elsewhere, which tends to make papers usually much more readable.

Corrected.

202: prior to

This was a typo, thank you.

213: allows estimating (or allows us to estimate)

Corrected.

227 equation numbering missing; please split into two equations (or substitute  $C_a = C_t + C_c$  into the first equation)

We adjust the second expression in this equation accordingly. The missing equation numbering is a typo; we did not intend to number this equation since we do not refer to it except within this paragraph.

227: *i* is not needed - can refer to any isotope.

Removed.

232: Eq. (2) does not match description in text below. Please rewrite the equation with  $\delta_a$  on the left hand side.

$$\delta_a = \delta_c + (\delta_t - \delta_c) * C_t / C_a$$

Since  $C_t$  is fixed and  $C_a$  is increasing with increasing  $C_c$  this also simplifies your discussion.

Thank you, we have reformulated this equation which has indeed simplified the discussion.

255: Please delete "It is noteworthy". Everything in the paper should be noteworthy, otherwise it should be removed.

Replaced with "It is important to note".

260-262: Unclear what you mean and the MM "does not ascertain results" - perhaps you are trying to say is that mixing model does provide any significant information on the  $\delta^{13}\text{C}$  value of the contamination?

Yes. We reformulate these statements as

Taking the same subsets of samples, the concomitant  $^{13}\text{C}$  signature matches  $^{13}\delta_c = -(23.3 \pm 8.6)\%$ , indeed at the upper end of the expected LMS  $\delta^{13}\text{C}(\text{CO})$  variations of  $-(25-31)\%$ . Because of that, the MM is likely insensitive to the changes in  $\delta^{13}\text{C}(\text{CO})$  caused by the contamination (the corresponding  $R^2$  values are below 0.1).

280: Expand MPI-C.

Expanded.

288-290: Unclear what "by conjecturing an inhibition of the formation KIEs proportional to that measured at  $\sim 320\text{ K}$ " means.

We replace this statement with "by assuming that the formation KIEs become attenuated at higher pressures in a similar (proportional) fashion to that measured at  $320\text{ K}$ ".

291: Unclear why this is missing - what does this refer to?

We reformulate this sentence as

A decrease in  $\delta^{18}\text{O}(\text{O}_3)$  of about  $(5.9-7.6)\%$  is expected from such calculation, yet accounting for a mere one-half of the  $(13.3-14.6)\%$  discrepancy between the stratospheric  $\delta^{18}\text{O}(\text{O}_3)$  values and  $^{18}\delta_c$ .

320,321: Add space between value and unit.

Added.

324: Merge unit with value, remove s-1.

We admit the use of square brackets is misleading here (as well as further in this paragraph), we correct these occurrences. However, the reported value is the reaction rate coefficient, which by definition has units of reciprocal number density per unit time. It is therefore unclear to us why “s<sup>-1</sup>” should be removed, or how the value can be merged with unit here. We propose using “(6·10<sup>-15</sup>/τ<sub>c</sub>) molec<sup>-1</sup> cm<sup>3</sup> s<sup>-1</sup>” instead. Alternatively, we will appreciate the Editor explicating this comment further.

327: There are no reactions that are this fast. Kinetic limit is about 2 x 10<sup>^(-10)</sup> cm<sup>3</sup> s<sup>-1</sup> (depends on the mass of the molecule).

Thank you. We change “rather high” to “unrealistically high” in this statement.

386: Write as m/z 45 (with m and z in italics - m/z this is a symbol, not a physical quantity; otherwise units would be required).

Corrected to “m/z”.

392: Please separate into two equations. What is this tilde/equal sign supposed to mean? Please show explicitly how you calculated the coefficient of 7.2568·10<sup>-2</sup> in the delta\_b equation with all values going into the calculation- the description is not clear.

We separate Eq. (B1) accordingly (see below). The tilde/equal sign “≅” was used to denote “approximately equal”; however, since this mathematical notation is not commonly used in ACP, we refrain from using it in the revised manuscript and explicitly state the approximation:

The respective bias <sup>13</sup>δ<sub>b</sub> is quantified using

$$^{13}\delta_b = 7.26 \cdot 10^{-2} \Delta^{17}\text{O}(\text{CO}), \quad (\text{B1})$$

where the actual Δ<sup>17</sup>O(CO) value is approximated from the natural CO MIF signal <sup>17</sup>Δ<sub>n</sub> and the typical O<sub>3</sub> MIF composition <sup>17</sup>Δ<sub>c</sub> as

$$\Delta^{17}\text{O}(\text{CO}) = ({}^{17}\Delta_n (C_a - C_c) + {}^{17}\Delta_c C_c)(C_a)^{-1}. \quad (\text{B2})$$

Regarding the calculation of the coefficient proportionating <sup>13</sup>δ<sub>b</sub> and Δ<sup>17</sup>O(CO), we used the calculation apparatus which is exhaustively described by Assonov and Brenninkmeijer (2001) and thus is out of the scope of this paper. We add, however, additional information which we believe is sufficient for the Reader to follow our calculations, namely:

The coefficient that proportionates <sup>13</sup>δ<sub>b</sub> and Δ<sup>17</sup>O in Eq. (B1) is reckoned by linearly regressing the δ<sup>13</sup>C(CO) biases (simulated using the calculation apparatus detailed by Assonov and Brenninkmeijer (2001)) as a function of Δ<sup>17</sup>O(CO) varying within a (0–30)‰ range for the CO with initially unaccounted MIF (e.g., the sample is assumed to be mass-dependently fractionated). It therefore quantifies some extra +(0.726±0.003)‰ in the analysed δ<sup>13</sup>C(CO) per every +10‰ of Δ<sup>17</sup>O(CO) excess.

393: What "remaining parameters"?

With this we implied the parameters C<sub>t</sub> and C<sub>c</sub> used in the calculations with the MM and derived in the contamination kinetic framework. We reformulate this statement (also in view of re-formulated Eq. (B2), see the answer to the previous comment) as follows:

Here C<sub>a</sub> and C<sub>c</sub> denote the analysed CO abundance and contamination magnitude, respectively, used in the contamination kinetic framework (see Appendix A, Eq. (A3)) and in calculations with the MM (see Sect. 3.1).

53 collected onboard a passenger aircraft carrying an airfreight container with analytical and  
54 air/aerosol sampling equipment on long distance flights from Germany to South India and the  
55 Caribbean within the framework of the CARIBIC project (Civil Aircraft for the Regular Invest-  
56 gation of the atmosphere Based on an Instrument Container, [http://www.caribic-  
57 atmospheric.com](http://www.caribic-atmospheric.com)).

## 58 2 Experimental and results

### 61 2.1 Whole air sampling

59 [4] CARIBIC-1 (Phase #1, abbreviated hereafter “C1”) was operational from November 1998  
60 until April 2002 using a *Boeing 767-300 ER* operated by LTU International Airlines  
61 (Brenninkmeijer *et al.*, 1999). Using a whole air sample (WAS) collection system, twelve air  
62 samples were collected per flight (of ~~8-10~~ hours duration at cruise altitudes of 10–12 km) in  
63 stainless steel tanks for subsequent laboratory analysis of the abundances of various trace gases,  
64 including  $^{14}\text{CO}$ . Large air samples were required in view of the ultra-low abundance of this  
65 mainly cosmogenic tracer (10–100 molecules  $\text{cm}^{-3}$  STP, about 40–400 amol/mol). (Hereinafter  
66 STP denotes dry air at 273.15 K, 101325 Pa.) Each C1 WAS sample (holding ~~350~~ litres of air  
67 STP) was collected within 15–20 min intervals representing the integral of the compositions  
68 encountered along flight segments of about 250 km. The overall uncertainty of the measured  
69 WAS  $\text{CO}_2$  is less than  $\pm 1\%$  for the mixing ratio and  $\pm 0.1\%/\pm 0.2\%$  for  $\delta^{13}\text{C}(\text{CO})/\delta^{18}\text{O}(\text{CO})$ , re-  
70 spectively (Brenninkmeijer, 1993; Brenninkmeijer *et al.*, 2001). Isotope compositions are re-  
71 ported throughout this manuscript using the so-called delta value  $\delta_i = (R/R_{\text{st}} - 1)$  relating the ratio  
72  $R$  of rare ( $^{13}\text{C}$ ,  $^{18}\text{O}$  or  $^{17}\text{O}$ ) over abundant isotopes of interest to the standard ratio  $R_{\text{st}}$ . These are  
73 V-SMOW of  $2005.20 \times 10^{-6}$  for  $^{18}\text{O}/^{16}\text{O}$  (Gonfiantini, 1978; Coplen, 1994) and  $386.72 \times 10^{-6}$  for  
74  $^{17}\text{O}/^{16}\text{O}$  (Assonov and Brenninkmeijer, 2003), and V-PDB of  $11237.2 \times 10^{-6}$  for  $^{13}\text{C}/^{12}\text{C}$   
75 (Craig, 1957), respectively. As we mention above, the oxygen isotopic composition of the CO  
76 present in these WAS samples was corrupted, in particular when  $\text{O}_3$  levels were as high as  
77 100–600 nmol/mol.

78 [5] CARIBIC-2 (Phase #2, referred to as “C2”) started operation in December 2004 with a  
79 Lufthansa *Airbus A340-600* fitted with a new inlet system and air sampling lines, including  
80 PFA lined tubing for trace gas intake (Brenninkmeijer *et al.*, 2007). No flask CO mixing/isotope  
81 ratio measurements are performed in C2.

Deleted: ~

Deleted: ~

Deleted: ~

Deleted: [

Deleted: ]

Deleted: '

Deleted: '

Deleted: '

Deleted: R

Deleted: ( $i$  denotes  $^{13}\text{C}$ ,  $^{18}\text{O}$  or  $^{17}\text{O}$ )

Deleted: '

## 2.2 On-line instrumentation

[6] In addition to the WAS collection systems, both C1 and C2 measurement setups include different instrumentation for on-line detection of [CO] and [O<sub>3</sub>] (hereinafter the squared brackets [] denote the abundance, *i.e.* concentration or mixing ratio, of the respective species). *In situ* CO analysis in C1 is done using a gas chromatography (GC)-reducing gas analyser which provides measurements every 130 s with uncertainty of ±3 nmol/mol (Zahn *et al.*, 2000). In C2, a vacuum ultraviolet fluorescence (VUV) instrument with lower measurement uncertainty and higher temporal resolution of ±2 nmol/mol in 2 s (Scharffe *et al.*, 2012) is employed, respectively. Furthermore, the detection frequency for O<sub>3</sub> abundance has also increased, *viz.* from 0.06 Hz in C1 to 5 Hz in C2 (Zahn *et al.*, 2002; Zahn *et al.*, 2012).

Deleted: each

Deleted: ~

Deleted: mixing ratio

## 2.3 Results

[7] When comparing the CO abundances in relation to those of O<sub>3</sub> for C1 and C2, differences are apparent in the LMS, where C2 CO values are systematically lower. This is illustrated in Fig. 1 (a) which presents the LMS CO-O<sub>3</sub> distribution of the C2 measurements overlaid with the C1 *in situ* and WAS data. (The entire C1 CO/O<sub>3</sub> dataset is presented in Fig. 2.) For the *in situ* CO datasets we calculated the statistics (Fig. 1 (b)) of the samples with respective O<sub>3</sub> abundances clustered in 20 nmol/mol bins, *i.e.* the median and spread of [CO] as a function of [O<sub>3</sub>] analysed. (The interquartile range, IQR, is used in the current analysis as a robust measure of the data spread instead of the standard deviation.) The data exhibit large [CO] variations at [O<sub>3</sub>] below 400 nmol/mol that primarily reflect pronounced seasonal variations in the NH tropospheric CO abundance. With O<sub>3</sub> rising, [CO] decreases to typical stratospheric values, and its spread reduces to mere 3.5 nmol/mol and less, as [O<sub>3</sub>] surpasses 500 nmol/mol. Despite the comparable spread in C1 and C2 [CO], from 400 nmol/mol of [O<sub>3</sub>] onwards the C1 CO mixing ratios start to level off, with no samples below 35 nmol/mol having been detected, whereas the C2 levels continuously decline. By the 580 nmol/mol O<sub>3</sub> bin, C1 [CO] of 39.7±0.3 nmol/mol accommodates some extra 15 nmol/mol compared to 25.6±1.7 nmol/mol typical for C2 values. Overall, at [O<sub>3</sub>] above 400 nmol/mol the conspicuously high [CO] is marked in about 200 *in situ* C1 samples, of which 158 and 69 emerge as statistically significant mild and extreme outliers, respectively, when compared against the ample ( $n \geq 3 \cdot 10^5$ ) C2 statistics. (The conventions here follow Natrella (2003), *i.e.* ±1.5 and ±3 IQR ranges define the inner and outer statistical fences (ranges outside which the data points are considered mild and extreme outliers) of the C2 [CO] distribution in every O<sub>3</sub> bin, respectively. The statistics include the samples in bins

Deleted: mixing ratios

Deleted: Error! Reference source not found., Panel

Deleted: increasingly becomes

Deleted: ~

Deleted: ; t



131 with average  $[O_3]$  of 420–620 nmol/mol.) None of C1 CO at  $[O_3]$  above 560 nmol/mol agrees  
132 with the C2 observations. Because the CO levels cannot have changed over the period in ques-  
133 tion by the difference we find (up to 55%), artefacts and calibration issues need to be scruti-  
134 nised.

135 [8] Unnatural elevations in the  $^{18}O/^{16}O$  ratios of CO from WAS measurements are also evident,  
136 as shown in Figs. 3 and 4. The large  $\delta^{18}O(CO)$  departures that reach beyond +16‰ are found to  
137 be proportional to the concomitant  $O_3$  abundances (denoted with colour) and more prominent at  
138 lower  $[CO]$ . A rather different relationship, however, is expected from our knowledge of UT/  
139 LMS CO sources (plus their isotope signatures) and available *in situ* observations (Fig. 2,  
140 shown with triangles), as elucidated by Brenninkmeijer *et al.* (1996) (hereafter denoted as  
141 “B96”). That is, the more stratospheric CO is, the greater fraction of its local inventory is re-  
142 filled with the photochemical component stemming from methane oxidation with a characteris-  
143 tic  $\delta^{18}O$  signature of ~0‰ or lower (Brenninkmeijer and Röckmann, 1997). This occurs because  
144 the CO sink at ruling UT/LMS temperatures proceeds more readily than its production, as the  
145 reaction of hydroxyl radical (OH) with CO, being primarily pressure-dependent, outcompetes  
146 the temperature-sensitive reaction of OH with  $CH_4$ . Furthermore, as the lifetime of CO quickly  
147 decreases with altitude, transport-mixing effects take the lead in determining the vertical distri-  
148 butions of  $[CO]$  and  $\delta^{18}O(CO)$  above the tropopause, hence their mutual relationship. This is  
149 seen from the B96 data at  $[CO]$  below 50 nmol/mol that line-up in a near linear relationship to-  
150 wards the end-members with lowest  $^{18}O/^{16}O$  ratios. These result from the largest share of the  
151  $^{18}O$ -depleted photochemical component and extra depletion caused by the preferential removal  
152 of  $C^{18}O$  in reaction with OH (fractionation about ~11‰ at pressures below 300 hPa, Ste-  
153 vens *et al.*, 1980; Röckmann *et al.*, 1998b).

154 [9] It is beyond doubt that the enhancements of C1  $C^{18}O$  originate from  $O_3$ , whose large en-  
155 richment in heavy oxygen (above +60‰ in  $\delta^{18}O$ , Brenninkmeijer *et al.*, 2003) is typical and  
156 found transferred to other atmospheric compounds (see Savarino and Morin (2012) for a re-  
157 view). In Fig. 2 it is also notable that not only the LMS compositions are affected but elevations  
158 of (3–10)‰ from the bulk  $\delta^{18}O(CO)$  values are present in more tropospheric samples with  $[CO]$   
159 of up to ~100 nmol/mol. These result from the dilution of the least affected CO-rich tropospheric  
160 air by CO-poor, however substantially contaminated, stratospheric air, sampled into the same  
161 WAS tank. Such sampling-induced mixing renders an unambiguous determination of the arte-  
162 fact source’ isotope signature rather difficult, because neither mixing nor isotope ratios of the  
163 admixed air portions are known sufficiently well (see below).

Deleted: Fig. 3

Deleted: (see also Fig. S2 in the Supplementary Material)

Deleted: *ibid.*

Deleted: with high mixing ratios

168 [10] Differences between the WAS and *in situ* measured [CO] – a possible indication that the  
 169  $\delta^{18}\text{O}(\text{CO})$  contamination pertains specifically to the WAS data – average at  $\bar{\Delta}(\text{WAS}-\textit{in situ}) =$   
 170  $(5.3 \pm 0.2)$  nmol/mol ( $\pm 1$  standard deviation, of the mean,  $n = 408$ ) and happen to be random with  
 171 respect to any operational parameter or measured characteristic in C1, *i.e.* irrespective of CO or  
 172  $\text{O}_3$  abundances. The above mentioned discrepancy remained after several calibrations between  
 173 the two systems had been performed, and likely results from the differences in the detection  
 174 methods, drifts of the calibration standards used (see details in Brenninkmeijer *et al.*, 2001) and  
 175 a short-term production of CO in the stainless steel tanks during sampling. The large spread of  
 176  $\Delta(\text{WAS}-\textit{in situ})$  of  $\pm 3.5$  nmol/mol ( $\pm 1\sigma$  of the population) ensues from the fact that the *in situ*  
 177 sampled air corresponds to (2–4)% of the concomitantly sampled WAS volume, as typically  
 178 6–7 *in situ* collections of  $\sim 5$  s were made throughout one tank collection of 17–21 min. The in-  
 179 tegrity of the WAS CO is further affirmed by the unsystematic distribution of the artefact com-  
 180 positions among tanks (an opposite case for  $\delta^{18}\text{O}(\text{CO}_2)$  in C1 is discussed by As-  
 181 sonov *et al.*, 2009). Overall, the WAS and *in situ* measured CO mixing ratios correlate extreme-  
 182 ly well (adj.  $R^2 = 0.972$ , slope of  $0.992 \pm 0.008$  ( $\pm 1\sigma$ ),  $n = 408$ ). However, both anomalies in  
 183 [CO] and  $\delta^{18}\text{O}(\text{CO})$  manifest clear but complex functions of the concomitant [ $\text{O}_3$ ]. That is, the  
 184 C1 *in situ* and WAS data very likely evidence artefacts pertaining to the  $\text{O}_3$ -driven effect of the  
 185 same nature. Below we ascertain and quantify these.

### 186 3 Discussion

187 [11] Three factors may lead to the (artefact) distributions such as seen for C1 *in situ* [CO] at the  
 188 LMS  $\text{O}_3$  abundances, namely:

189 [12] (i) Strong (linear) natural mixing, such as enhanced stratosphere-troposphere exchange  
 190 (STE), when a [CO] outside the statistically expected range results from the integration of air  
 191 having dissimilar ratios of the tracers' abundances, *viz.* [ $\text{O}_3$ ]:[CO]. For example, mixing of two  
 192 air parcels in a 15%:85% proportion (by moles of air) with typical [ $\text{O}_3$ ]:[CO] of 700:24 (strato-  
 193 spheric) and 60:125 (tropospheric), respectively, yields an integrated composition with  
 194 [ $\text{O}_3$ ]:[CO] of  $\sim 580:40$  which indeed corresponds to C1 data (this case is exemplified by the mix-  
 195 ing curve in Fig. 1). Nonetheless, occurrences of rather high (compared to the typical  
 196 24–26 nmol/mol) stratospheric CO mixing ratios (in our case,  $\sim 40$  nmol/mol at the concomitant  
 197 [ $\text{O}_3$ ] of 500–600 nmol/mol) are rare. For instance, a deep STE similar to that described by  
 198 Pan *et al.* (2004) was observed by C2 only once (*cf.* the outliers at [ $\text{O}_3$ ] of 500 nmol/mol in  
 199 Fig. 1), whereas the C1 outliers were exclusively registered in some 12 flights during

Deleted: WAS

Formatted: Not Superscript/ Subscript

Deleted: *in situ*

Formatted: Not Superscript/ Subscript

Deleted: SD

Deleted: quoted mixing ratio

Deleted: WAS-*in situ*

Deleted: ~

Deleted:  $\rho_{\text{O}_3:\text{CO}} =$

Deleted: /

Deleted:  $\rho_{\text{O}_3:\text{CO}}$

Deleted:  $\rho_{\text{O}_3:\text{CO}}$

210 1997–2001. No relation between these outliers and the large-scale [CO] perturbation due to ex-  
211 tensive biomass burning in 1997/1998 (Novelli *et al.*, 2003) is established, otherwise elevated  
212 CO mixing ratios should manifest themselves at lower [O<sub>3</sub>] as well. Other tracers detected in  
213 CARIBIC provide supporting evidence against such strongly STE-mixed air having been cap-  
214 tured by C1. That is, the binned distributions for the water vapour and de-trended N<sub>2</sub>O (similar  
215 to that for [CO] vs. [O<sub>3</sub>] presented in Fig. 1, not shown here) are greatly similar in C1 and C2.  
216 Whereas the small relative variations in atmospheric [N<sub>2</sub>O] merely confirm matching [O<sub>3</sub>] sta-  
217 tistics in CARIBIC, the stratospheric [H<sub>2</sub>O] distributions witness no [O<sub>3</sub>]:[CO] values corre-  
218 sponding to those of the C1 outliers, suggesting the latter being unnaturally low.

Deleted:  $\rho_{O_3:H_2O}$

Deleted: ' $\rho_{O_3:CO}$

219 [13] (ii) Mixing effects can also occur artificially, originating from sampling peculiarities or data  
220 processing. Since the CARIBIC platform is not stationary, about 5 s long sampling of an *in situ*  
221 air probe in C1 implies integration of the compositions encountered along some hundred met-  
222 res, owing to the high aircraft speed. This distance may cover a transect between tropospheric  
223 and stratospheric filaments of much different compositions. The effect of such ‘translational  
224 mixing’ can be simulated by averaging the sampling data with higher temporal frequency over  
225 longer time intervals. In this respect, the substantially more frequent CO data in C2 (<1 s) were  
226 artificially averaged over a set of increasing intervals to reckon whether the long sampling peri-  
227 od in C1 could be the culprit for skewing its CO–O<sub>3</sub> distribution. As a result, the original C2 da-  
228 ta and their averages (equivalent to the C1 CO sample injection time) differ negligibly, as do  
229 the respective [O<sub>3</sub>]:[CO] values. The actual C2 CO–O<sub>3</sub> statistic in the region of interest ([O<sub>3</sub>] of  
230 540–620 nmol/mol) remains insensitive to integration of up to 300 s. Furthermore, a very  
231 strong artificial mixing with an averaging interval of at least 1200 s (comparable to C1 WAS  
232 sampling time) is required to yield the averages from the C2 data with [O<sub>3</sub>]:[CO] characteristic  
233 for the C1 outliers.

Deleted:  $\rho_{O_3:CO}$

Deleted: ; t

Deleted:  $\rho_{O_3:CO}$

234 [14] (iii) In view of the above, it is unlikely that any natural or artificial mixing processes are in-  
235 volved in the stratospheric [CO] discrepancies seen in C1. We therefore conclude that the sam-  
236 ple contamination in C1 occurred prior to the probed air reaching the analytical/sampling in-  
237 strumentation in the container, since clearly elevated stratospheric CO mixing ratios are com-  
238 mon to WAS and *in situ* data. Two more indications, *viz.* growing [CO] discrepancy with in-  
239 creasing O<sub>3</sub> abundance, and the strong concomitant signal in  $\delta^{18}O(CO)$ , imply that O<sub>3</sub>-mediated  
240 photochemical production of CO took place. Further, by confronting the C1 and C2 [CO] meas-  
241 urements in a kinetic framework (detailed in Appendix A), we quantify the artefact CO compo-  
242 nent being chiefly a function of O<sub>3</sub> abundance as

Deleted: It

Deleted: stands to reason to

$$C_c = b \cdot [\text{O}_3]^2, b = (5.19 \pm 0.12) \cdot 10^{-5} \text{ [mol/nmol]}, \quad (1)$$

which is equivalent to 8–18 nmol/mol throughout the respective  $[\text{O}_3]$  range of 400–620 nmol/mol (see Fig. 1 (d)). Subtracting this artefact signal yields the corrected *in situ* C1 CO–O<sub>3</sub> distribution conform to that of C2 (*cf.* red symbols in Fig. 1 (a)).

[15] Importantly, since we can quantify the contamination strength using only the O<sub>3</sub> abundance, the continuous *in situ* C1 [O<sub>3</sub>] data allows estimating the integral artefact CO component in each WAS sample and, if the isotope ratio of contaminating O<sub>3</sub> is known, to derive the initial  $\delta^{18}\text{O}(\text{CO})$ . The latter, as it was mentioned above, is subject to strong sample-mixing effects, which is witnessed by  $\delta^{18}\text{O}(\text{CO})$  outliers even at relatively high [CO] up to 100 nmol/mol. Accounting for such cases is, however, problematic since it is necessary to distinguish the proportions of the least modified (tropospheric) and significantly affected (stratospheric) components in the resultant WAS sample mix. In reality, however, this information is not available, therefore we applied an *ad hoc* correction approach (which is capable of determining the contamination source (*i.e.*, O<sub>3</sub>) isotope signature as well), as described in the following.

### 3.1 Contamination isotope signatures

[16] Practically we resort to the differential mixing model (MM, originally known as the “Keeling-plot”), because it requires only the estimate of the artefact component mixing ratio, but no assumptions on the (unknown) shares and isotope signatures of the air portions mixed in a given WAS tank. The MM parameterises the admixing of the portion of artefact CO to the WAS sample with the “true” initial composition, as formulated below:

$$\begin{cases} \delta_a C_a = C_t \delta_t + C_c \delta_c, \\ C_a \equiv C_t + C_c \end{cases},$$

where indices  $a$ ,  $c$  and  $t$  distinguish the abundances  $C$  and isotope compositions  $\delta$  (<sup>13</sup>C and <sup>18</sup>O) pertaining to the analysed sample, estimated contamination and “true” composition sought (*i.e.*,  $C_t$  and  $\delta_t$ ), respectively. (Here the contamination strength  $C_c$  is derived by integrating Eq. (1) using the *in situ* C1 [O<sub>3</sub>] data for each WAS sample.) By rewriting the above equation with respect to the isotope signature of the analysed CO, one obtains:

$$\delta_a = \delta_c + (\delta_t - \delta_c) C_t / C_a, \quad (2)$$

which signifies that linear regression of  $\delta_a$  as a function of the reciprocal of  $C_a$  yields the estimated contamination signature  $\delta_c$  at  $(C_a)^{-1} \rightarrow 0$  when invariable “true” compositions ( $C_t$ ,  $\delta_t$ ) are taken (the Keeling plot detailing these calculations is shown in Fig. 5). We therefore apply the

Deleted: to

Deleted: e

Deleted: . ()

Deleted: ‘

Deleted:  $i$  may refer to

Deleted: or

Deleted: ‘

Deleted: .

Deleted: .

Deleted: .

Deleted: admixed portion

Deleted:  $\delta_c$ .

Deleted: the measured ‘

Deleted:  $c$ .

Deleted: ‘

Deleted:  $c$ .

Deleted: (The Keeling plot detailing the calculations with the MM is shown in Supplementary Material, Fig. S3.) The MM described by Eq. (2) provides adequate results only for the invariable initial compositions ( $C_t$ ,  $\delta_t$ ),

Deleted: we

296 MM described by Eq. (2), to the subsets of samples picked according to the same reckoned  $C_i$   
297 (within a  $\pm 2$  nmol/mol window,  $n > 7$ ). Such selection, however, may be insufficient: Due to the  
298 strong sampling effects in the WAS samples (see previous Section), it is possible to encounter  
299 samples that integrate different air masses to the same  $C_i$  but rather different average  $\delta_i$ . The so-  
300 lution in this case is to refer to the goodness of the MM regression fit, because the  $R^2$  intrin-  
301 sically measures the linearity of the regressed data, *i.e.* closeness of the “true” values in a regard-  
302 ed subset of samples, irrespective of underlying reasons for that.

303 [17] Higher  $R^2$  values thus imply higher consistency of the estimate, as demonstrated in Fig. 6  
304 showing the calculated  $\delta_c$  for  $C_i$  below 80 nmol/mol as a function of the regression  $R^2$ . The lat-  
305 ter decreases with greater  $C_i$  (*i.e.*, larger sample subset size, since tropospheric air is more often  
306 encountered) and, conformably, larger variations in  $\delta_c$ . Ultimately, at lower  $R^2$  the inferred  $^{18}\text{O}$   
307 signatures converge to values slightly above zero expected for uncorrelated data, *i.e.* C1  
308  $\delta^{18}\text{O}(\text{CO})$  tropospheric average. A similar relationship is seen for the  $^{13}\text{C}$  signatures (they con-  
309 verge around  $-28\text{‰}$ ), however, there are no consistent estimates found ( $R^2$  is generally below  
310 0.4). Since such is not the case for  $\delta^{18}\text{O}$ , the MM is not sufficiently sensitive to the changes  
311 caused by the contamination, which implies that the artefact CO  $\delta^{13}\text{C}$  should be within the  
312 range of the “true”  $\delta^{13}\text{C}(\text{CO})$  values. Interestingly, the MM is rather responsive to the growing  
313 fraction of the  $\text{CH}_4$ -derived component in CO with increasing  $[\text{O}_3]$ , as the  $^{13}\delta_c$  value of  
314  $(-47.2 \pm 5.8)\text{‰}$  inferred at  $R^2$  above 0.4 is characteristic for the  $\delta^{13}\text{C}$  of methane in the UT/LMS.  
315 It is **important to note** that we have accounted for the biases in the analysed C1 WAS  $\delta^{13}\text{C}(\text{CO})$   
316 expected from the mass-independent isotope composition of  $\text{O}_3$  (see details in Appendix B).

317 [18] We derive the “best-guess” estimate of the admixed CO  $^{18}\text{O}$  signature at  $^{18}\delta_c =$   
318  $(+92.0 \pm 8.3)\text{‰}$ , which agrees with the other MM results obtained at  $R^2$  above 0.75. Taking the  
319 same subsets of samples, the concomitant  $^{13}\text{C}$  signature matches  $^{13}\delta_c = (-23.3 \pm 8.6)\text{‰}$ , indeed at  
320 the upper end of the expected LMS  $\delta^{13}\text{C}(\text{CO})$  variations of  $(-25\text{--}31)\text{‰}$ . **Because of that**, the  
321 MM **is likely insensitive** to the **changes in  $\delta^{13}\text{C}(\text{CO})$  caused by the** contamination (the corre-  
322 sponding  $R^2$  values are below 0.1). Upon the correction using the inferred  $^{18}\delta_c$  value, the C1  
323 WAS  $\delta^{18}\text{O}(\text{CO})$  data appear adequate (shown with red symbols in Fig. 2). That is, variations in  
324 the observed  $\text{C}^{18}\text{O}$  are driven by (i) the seasonal/regional changes in the composition of tropo-  
325 spheric air and by (ii) the degree of mixing or replacement of the latter with the stratospheric  
326 component that is less variable in  $^{18}\text{O}$ . This is seen as stretching of the scattered tropospheric  
327 values ( $[\text{CO}]$  above 60 nmol/mol) in a mixing fashion towards  $\delta^{18}\text{O}(\text{CO})$  of around  $-10\text{‰}$  at  
328  $[\text{CO}]$  of  $\sim 25$  nmol/mol, respectively. The corrected C1  $\delta^{13}\text{C}(\text{CO})$  data (shown in Fig. 7) are

Deleted: it

Deleted: ‘

Deleted: ‘

Deleted: ‘

Deleted:  $^{13}\text{C}$

Deleted: worthy

Deleted:  $^{18}\text{O}$

Deleted:  $^{13}\text{C}$

Deleted: , which

Deleted: likely does not allow

Deleted: to ascertain this result as pertaining

Deleted:  $^{18}\text{O}$

Deleted: Supplementary Material, Fig. S4

342 found to be in a  $\pm 1\%$  agreement with the observations by B96, except for several deep strato-  
343 spheric samples ([CO] below 40 nmol/mol). The latter were encountered during "ozone hole"  
344 conditions and carried extremely low  $^{13}\text{C}$ O abundances, which was attributed to the reaction of  
345 methane with available free Cl radicals (Brenninkmeijer *et al.*, 1996).

### 3.2 Estimate of $\delta^{18}\text{O}(\text{O}_3)$

346 [19] The contamination  $^{18}\text{O}_\text{c}$  signature inferred here ( $\delta^{18}\text{O}_\text{c} = +(92.0 \pm 8.3)\%$ ) unambiguously per-  
347 tains to  $\text{O}_3$  and is comparable to  $\delta^{18}\text{O}(\text{O}_3)$  values measured in the stratosphere at temperatures  
348 about 30 K lower than those encountered in the UT/LMS by C1 (see Table 1 for comparison). If  
349 no other factors are involved (see below), this discrepancy in  $\delta^{18}\text{O}(\text{O}_3)$  should be attributed to  
350 the local conditions, *i.e.* the higher pressures (typically 240–270 hPa for C1 cruising altitudes)  
351 at which  $\text{O}_3$  was formed. Indeed, the molecular lifetime (the period through which the species'  
352 isotope reservoir becomes entirely renewed, as opposed to the "bulk" lifetime) of  $\text{O}_3$  encoun-  
353 tered along the C1 flight routes is estimated on the order of minutes to hours at daylight  
354 (H. Riede, Max Planck Institute for Chemistry, 2010), thus the isotope composition of the pho-  
355 tochemically regenerated  $\text{O}_3$  resets quickly according to the local conditions. Virtual absence of  
356 sinks, in turn, leads to "freezing" of the  $\delta^{18}\text{O}(\text{O}_3)$  value during night in the UT/LMS. Verifying  
357 the current  $\delta^{18}\text{O}(\text{O}_3)$  estimate against the kinetic data, in contrast to the stratospheric cases, is  
358 problematic. The laboratory studies on  $\text{O}_3$  formation to date have scrutinised the concomitant  
359 kinetic isotope effects (KIEs) as a function of temperature at only low pressures (50 Torr); the  
360 attenuation of the KIEs with increasing pressure was studied only at room temperatures (see  
361 Table 1, also Brenninkmeijer *et al.* (2003) for references). A rather crude attempt may be under-  
362 taken by assuming that the formation KIEs become attenuated at higher pressures in a similar  
363 (proportional) fashion to that measured at 320 K, however applied to the nominal low-pressure  
364 values reckoned at (220–230)K. A decrease in  $\delta^{18}\text{O}(\text{O}_3)$  of about (5.9–7.6)% is expected from  
365 such calculation, yet accounting for a mere one-half of the (13.3–14.6)% discrepancy between  
366 the stratospheric  $\delta^{18}\text{O}(\text{O}_3)$  values and  $\delta^{18}\text{O}_\text{c}$ .

367 [20] Lower  $\delta^{18}\text{O}_\text{c}$  values could result from possible isotope fractionation accompanying the pro-  
368 duction of the artefact CO. Although not quantifiable here, oxygen KIEs in the  $\text{O}_3 \rightarrow \text{CO}$  con-  
369 version chain cannot be ruled out, recalling that the intermediate reaction steps are not identifi-  
370 able and the artefact CO represents at most 4% of all  $\text{O}_3$  molecules. Furthermore, the yield  $\lambda_{\text{O}_3}$   
371 of CO from  $\text{O}_3$  may be lower than unity (see details in Appendix A). On the other hand, the in-  
372 ference that the contamination strength primarily depends on  $[\text{O}_3]$  indicates that the kinetic frac-

Deleted:  $^{18}$

Deleted:  $^{18}\text{O}_\text{c}$

Deleted:  $^{18}$

Deleted:  $^0$

Deleted: -

Deleted: conjecturing

Deleted: an inhibition of

Deleted: ~

Deleted: "missing" in

Deleted:  $^{18}$

Deleted:  $^0$

Deleted:  $^{18}$

Deleted:  $^0$

386 tionation may have greater effect on the carbon isotope ratios of the artefact CO produced (the  
387  $\delta^{13}\text{C}_c$  values) in contrast to the oxygen ones. That is because all reactive oxygen available from  
388  $\text{O}_3$  becomes converted to CO, whilst the concomitant carbon atoms are drawn from a virtually  
389 unlimited pool whose apparent isotope composition is altered by the magnitude of the  $^{13}\text{C}$  KIEs.

390 [21] Besides KIEs, selectivity in the transfer of O atoms from  $\text{O}_3$  to CO affects the resulting  $\delta^{18}\text{O}_c$   
391 value. The terminal O atoms in  $\text{O}_3$  are enriched with respect to the molecular (bulk)  $\text{O}_3$  compo-  
392 sition when the latter is above  $\sim 70\%$  in  $\delta^{18}\text{O}$  (Janssen, 2005; Bhattacharya *et al.*, 2008), there-  
393 fore an incorporation of only central O atoms into the artefact CO molecules should result in a  
394 reduced apparent  $\delta^{18}\text{O}_c$  value. Such exclusive selection is, however, less likely from the kinetic  
395 standpoint and was not observed in available laboratory studies (see Savarino *et al.* (2008) for a  
396 review). For instance, Röckmann *et al.* (1998a) established the evidence of direct O transfer  
397 from  $\text{O}_3$  to the CO produced in alkene ozonolysis. A reanalysis of their results (in light of find-  
398 ings of Bhattacharya *et al.* (2008)) suggests that usually the terminal atoms of the  $\text{O}_3$  molecule  
399 become transferred (their ratio over the central ones changes from the bulk  $\sim 2:1$  to  $\sim 1:0$  for var-  
400 ious species). Considering the alternatives of the O transfer in our case (listed additionally in  
401 Table 1), the equiprobable incorporation of the terminal and central  $\text{O}_3$  atoms into CO should  
402 result in the  $\delta^{18}\text{O}(\text{O}_3)$  value in agreement with the “crude” estimate based on laboratory data  
403 given above.

404 [22] Furthermore, the conditions that supported the reaction of  $\text{O}_3$  (or its derivatives) followed by  
405 the production of CO are vague. A few hypotheses ought to be scrutinised here. First, a fast  
406  $\text{O}_3 \rightarrow \text{CO}$  conversion must have occurred, owing to short (*i.e.*, fraction of a second) exposure  
407 time of the probed air to the contamination. Accounting for the typical C1 air sampling condi-  
408 tions (these are: sampled air pressure of 240–270 hPa and temperature of 220–235 K outboard  
409 to 275–300 K inboard, sampling rate of  $\sim 12.85 \cdot 10^{-3}$  moles  $\text{s}^{-1}$  corresponding to 350 L STP  
410 sampled in 1200 s, inlet/tubing volume gauged to yield exposure times of 0.01 to 0.1 s due to  
411 variable air intake rate,  $[\text{O}_3]$  of 600 nmol/mol), the overall reaction rate coefficient ( $k_c$  in  
412 Eq. (A1) from Appendix A) must be on the order of  $(6 \cdot 10^{-15}/\tau_c)$   $\text{molec}^{-1} \text{cm}^3 \text{s}^{-1}$ , where  $\tau_c$  is the  
413 exposure time. Assuming the case of a gas-phase CO production from a recombining  $\text{O}_3$  deriva-  
414 tive and an unknown carbonaceous compound X, the reaction rate coefficient for the latter ( $^Xk_r$   
415 in Eq. (A1) in Appendix A) must be unrealistically high, at least  $\sim 6 \cdot 10^{-10}$   $\text{molec}^{-1} \text{cm}^3 \text{s}^{-1}$  over  
416  $\tau_c = 1/100$  s. This number decreases proportionally with growing  $\tau_c$  and  $[\text{X}]$ , if we take less strict  
417 exposure conditions. Nonetheless, in order to provide the amounts of artefact CO we detect, a

Deleted: <sup>13</sup>

Deleted: <sup>c</sup>

Deleted: <sup>18</sup>

Deleted: <sup>o</sup>

Deleted: .

Deleted: .

Deleted: .

Deleted: to

Deleted: <sup>18</sup>

Deleted: <sup>o</sup>

Deleted: [

Deleted: ]

Deleted: rather

Deleted: [

Deleted: ]

433 minimum abundance of 20 nmol/mol (or up to 4  $\mu\text{g}$  of C per flight) of X is required, which is  
434 not available in the UT/LMS from the species readily undergoing ozonolysis, *e.g.* alkenes.

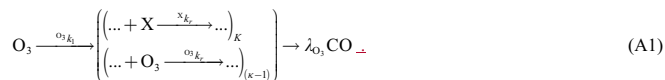
435 [23] Second, a more complex heterogeneous chemistry on the inner surface of the inlet or sup-  
436 plying tubing may be involved. Such can be the tracers' surface adsorption, (catalytic) decom-  
437 position of  $\text{O}_3$  and its reaction with organics or with surface carbon that also may lead to the  
438 production of CO (Oyama, 2000). Evidence exists for the dissociative adsorption of  $\text{O}_3$  on the  
439 surfaces with subsequent production of the reactive atomic oxygen species (see, *e.g.*,  
440 Li *et al.*, 1998, also Oyama, 2000). It is probable that sufficient amounts of organics have re-  
441 mained on the walls of the sampling line exposed to highly polluted tropospheric air, to be later  
442 broken down by the products of the heterogeneous decomposition of the ample stratospheric  $\text{O}_3$ .  
443 Unfortunately, the scope for a detailed quantification of intricate surface effects in the C1 CO  
444 contamination problem is very limited.

## 445 4 Conclusions

446 [24] Recapitulating, the *in situ* measurements of CO and  $\text{O}_3$  allowed us to unambiguously quanti-  
447 fy the artefact CO production from  $\text{O}_3$  likely in the sample line of the CARIBIC-1 instrumenta-  
448 tion. Strong evidence to that is provided by the isotope CO measurements. We demonstrate the  
449 ability of the simple mixing model ("Keeling-plot" approach) to single out the contamination  
450 isotope signatures even in the case of a large sampling-induced mixing of the air with very dif-  
451 ferent compositions. Obtained as a collateral result, the estimate of the  $\delta^{18}\text{O}(\text{O}_3)$  in the UT/LMS  
452 appears adequate, calling, however, for additional laboratory data (*e.g.*, the temperature-driven  
453 variations of the  $\text{O}_3$  formation KIE at pressures above 100 hPa) for a more unambiguous verifi-  
454 cation.

## 455 Appendix A. Contamination kinetic framework

456 [25] We infer the functional dependence of the CO contamination strength in the kinetic frame-  
457 work conceptually formulated as follows:



458 Eq. (A1) reads that production of an artefact CO molecules is initiated by  $\text{O}_3$  (via either its de-  
459 composition or a reaction with an unknown educt) and is followed by a set of unknown reac-

Deleted:  $\text{O}_3$ -exclusive

Deleted: C, by discriminating the C1 outliers from respective C2 data

Deleted: following



tions which proceed via unknown educts or products (denoted with ellipses), however requiring at some step an incorporation of carbon (donated by carbonaceous species X) and oxygen (also possible in secondary O<sub>3</sub> reactions) atoms into final CO. Coefficients K and κ describe the stoichiometry of the system, i.e. how many reactions of X and O<sub>3</sub> (with the individual unknown rate coefficients <sup>X</sup>k<sub>r</sub> and <sup>O<sub>3</sub></sup>k<sub>r</sub>) lead to production of one artefact CO, respectively. The yield λ<sub>O<sub>3</sub></sub>, a diagnostic quantity, relates the amount of artefact CO molecules produced to the total number of O<sub>3</sub> molecules consumed in the system. Based on Eq. (A1), the functional dependence of the artefact CO component (denoted C<sub>c</sub>, obtained by discriminating the C1 outliers from respective C2 data) on [O<sub>3</sub>] or [X] is generally formulated as (abundances in number density units are used)

$$C_c = \int_{\tau_c} \prod_{\kappa} \text{}^{\text{O}_3} k_r [\text{O}_3] \prod_K \text{}^{\text{X}} k_r [\text{X}] dt \quad \text{(A2)}$$

where τ<sub>c</sub> denotes the contamination reaction time. Eq. (A2) defines the regression expression using which we attempted to fit the values of C<sub>c</sub> as a function of κ, [O<sub>3</sub>], K and [X] (the latter was chosen iteratively from a set of carbonaceous species measured). Practically, however, this regression analysis ascertains that variations in C<sub>c</sub> are exhaustively described using [O<sub>3</sub>] and κ. Furthermore, we find that no other species or operational parameter (e.g. temperature, pressure, flight duration, latitude, etc.) measured in C1 appear to determine (correlate with) C<sub>c</sub>. Based on this, we can reduce Eq. (A2) to its final, simpler form, viz.

$$C_c = \lambda_{\text{O}_3} k_c [\text{O}_3]^\kappa \tau_c \quad \text{(A3)}$$

where k<sub>c</sub> denotes the overall pseudo-first-order rate coefficient of the reaction chain that is exclusively propelled by O<sub>3</sub>. The product (λ<sub>O<sub>3</sub></sub> k<sub>c</sub> τ<sub>c</sub>) thus integrates the influence of the unknown (and likely invariable) [X], <sup>X</sup>k<sub>r</sub>, K and τ<sub>c</sub>. Finally, regressing C<sub>c</sub> using Eq. (A3) provides its best approximation as a function of [O<sub>3</sub>] at κ = 2.06 ± 0.38, suggesting two chain steps involving O<sub>3</sub> or its derivatives. At κ = 2, the product (λ<sub>O<sub>3</sub></sub> k<sub>c</sub> τ<sub>c</sub>) that proportionates the CO contamination strength and [O<sub>3</sub>] is found to be (5.19 ± 0.12) · 10<sup>-5</sup> mol/nmol (±1σ, adj. R<sup>2</sup> = 0.83, red. χ<sup>2</sup> = 4.0; mole fraction units are used here for convenience). The low uncertainty (within ±3%) of this estimate confirms an exclusive dependence of the contamination source on the O<sub>3</sub> abundance, as well as much similar reaction times τ<sub>c</sub>. The regressed value of C<sub>c</sub> as a function of [O<sub>3</sub>] is presented in Fig. 1 (d) (solid line). It is possible to constrain the overall yield λ<sub>O<sub>3</sub></sub> of CO molecules in the artefact source chain to be between 0.5 and 1, comparing the magnitude of C<sub>c</sub> to the discrepancy between the [O<sub>3</sub>] measured in C1 and C2 (±20 nmol/mol, taken equal to the [O<sub>3</sub>] bin

Deleted: that

Deleted: or

Deleted:

Deleted: we find

Deleted: ,

Deleted: and k<sub>c</sub> (the latter are obtained in a regression analysis), where

Deleted: leading to the artefact CO production with the respective yield λ<sub>O<sub>3</sub></sub>. The individual rate coefficients <sup>X</sup>k<sub>r</sub> and <sup>O<sub>3</sub></sup>k<sub>r</sub> pertain to the unknown compound(s) X and O<sub>3</sub> reacting with the integral stoichiometry factors K and κ, respectively.

Deleted: value of

Deleted: K

Deleted: the

Deleted: o

Deleted: based on The relation defined by

Deleted: (A1)

Deleted: the

Deleted: for

Deleted: C<sub>c</sub>

Deleted: ratio C<sub>c</sub>/[O<sub>3</sub>]<sup>κ</sup> (essentially

Deleted: 1 to the reaction time τ<sub>c</sub> and overall rate coefficient k<sub>c</sub>

Deleted: )

Deleted: signifies

517 size owing to the N<sub>2</sub>O–O<sub>3</sub> and H<sub>2</sub>O–O<sub>3</sub> distributions matching well between the datasets). Lower  
 518  $\lambda_{O_3}$  values, otherwise, should have resulted in a noticeable (*i.e.*, greater than 20 nmol/mol)  
 519 decrease in the C1 O<sub>3</sub> abundances with respect to the C2 levels.

## 520 Appendix B. Corrections to measured $\delta^{13}\text{C}(\text{CO})$ values due to the oxygen 521 MIF

522 [26] Atmospheric O<sub>3</sub> carries an anomalous isotope composition (or mass-independent fractionation,  
 523 MIF) with a substantially higher relative enrichment in <sup>17</sup>O over that in <sup>18</sup>O (above +25‰  
 524 in  $\Delta^{17}\text{O} = (\delta^{17}\text{O}+1)/(\delta^{18}\text{O}+1)^{\beta}-1$ ,  $\beta = 0.528$ ) when compared to the majority of terrestrial oxy-  
 525 gen reservoirs that are mass-dependently fractionated (*i.e.*, with  $\Delta^{17}\text{O}$  of ~0‰) (see Brennink-  
 526 meijer *et al.* (2003) and refs. therein). CO itself also has an unusual oxygen isotopic composi-  
 527 tion, possessing a moderate tropospheric MIF of around +5‰ in  $\Delta^{17}\text{O}(\text{CO})$  induced by the sink  
 528 KIEs in reaction of CO with OH (Röckmann *et al.*, 1998b; Röckmann *et al.*, 2002) and a minor  
 529 source effect from the ozonolysis of alkenes (Röckmann *et al.*, 1998a; Gromov *et al.*, 2010). A  
 530 substantial contamination of CO by O<sub>3</sub> oxygen induces proportional changes to  $\Delta^{17}\text{O}(\text{CO})$  that  
 531 largely exceed its natural atmospheric variation. On the other hand, the MIF has implications in  
 532 the analytical determination of  $\delta^{13}\text{C}(\text{CO})$ , because the presence of C<sup>17</sup>O species interferes with  
 533 the mass-spectrometric measurement of the abundances of <sup>13</sup>CO possessing the same basic mo-  
 534 lecular mass ( $m/z$  is 45). When inferring the exact C<sup>17</sup>O/C<sup>18</sup>O ratio in the analysed sample is not  
 535 possible, analytical techniques usually involve assumptions (*e.g.*, mass-dependently fractionated  
 536 compositions or a certain non-zero  $\Delta^{17}\text{O}$  value) with respect to the C<sup>17</sup>O abundances  
 537 (Assonov and Brenninkmeijer, 2001). In effect for the C1 CO data, the artefact CO produced  
 538 from O<sub>3</sub> had contributed with unexpectedly high C<sup>17</sup>O abundances that led to the overestimated  
 539  $\delta^{13}\text{C}(\text{CO})$  analysed. The respective bias  $^{13}\delta_b$  is quantified using

$$^{13}\delta_b = 7.26 \cdot 10^{-2} \Delta^{17}\text{O}(\text{CO}), \quad (\text{B1})$$

540 where the actual  $\Delta^{17}\text{O}(\text{CO})$  value is approximated from the natural CO MIF signal  $^{17}\Delta_c$  and the  
 541 typical O<sub>3</sub> MIF composition  $^{17}\Delta_o$  as

$$\Delta^{17}\text{O}(\text{CO}) = (^{17}\Delta_c (C_o - C_c) + ^{17}\Delta_o C_c) (C_c)^{-1} \quad (\text{B2})$$

542 Here  $C_o$  and  $C_c$  denote the analysed CO abundance and contamination magnitude, respectively,  
 543 used in the contamination kinetic framework (see Appendix A, Eq. (A3)) and in calculations  
 544 with the MM (see Sect. 3.1). For the purpose of the current estimate it is sufficient to take  $^{17}\Delta_o$   
 545 of +5‰ representing equilibrium enrichments expected in the remote free troposphere and UT/

- Deleted: Furthermore
- Deleted: e
- Deleted: Knowing the contamination magnitude  $C_c$  and assuming the typical O<sub>3</sub> MIF composition being  $^{17}\text{O}^{17}\Delta_o$ , t
- Deleted: <sup>13</sup>C
- Deleted: calculated
- Deleted: 568
- Deleted: <sup>17</sup>O
- Deleted: ,
- Deleted: denotes the natural, *i.e.* expected "true" value of  $\Delta^{17}\text{O}(\text{CO})$ .
- Deleted: ,
- Deleted: ,
- Deleted: ,
- Deleted: The remaining parameters
- Deleted:  $C_c$  and
- Deleted: in Eq. (B2)
- Deleted: s
- Deleted: and  $C_c$  equals estimated,
- Deleted: reckoned
- Deleted: derived
- Deleted: the pertain
- Deleted: to

565 LMS. For the O<sub>3</sub> MIF signature  $^{17}\Delta_c$ , the value of +30‰ (the average  $\Delta^{17}\text{O}(\text{O}_3)$  expected from  
566 the kinetic laboratory data at conditions met along the C1 flight routes, see Sect. 3.2 and Ta-  
567 ble 1) is adopted. The coefficient that proportionates  $\delta^{13}\text{C}$  and  $\Delta^{17}\text{O}$  in Eq. (B1) is derived by lin-  
568 early regressing the  $\delta^{13}\text{C}(\text{CO})$  biases (simulated using the calculation apparatus detailed by  
569 Assonov and Brenninkmeijer, 2001) as a function of  $\Delta^{17}\text{O}(\text{CO})$  varying within a (0–30)‰  
570 range for the CO with initially unaccounted MIF (e.g., the sample is assumed to be mass-  
571 dependently fractionated). It therefore quantifies some extra  $+ (0.726 \pm 0.003)\%$  in the analysed  
572  $\delta^{13}\text{C}(\text{CO})$  per every +10‰ of  $\Delta^{17}\text{O}(\text{CO})$  excess. The most contaminated C1 WAS CO samples  
573 at [O<sub>3</sub>] above 300 nmol/mol are estimated to bear  $\Delta^{17}\text{O}(\text{CO})$  of (6–12)‰ corresponding to frac-  
574 tions of (0.10–0.27) of the artefact CO in the sample. Accordingly, the reckoned  $\delta^{13}\text{C}(\text{CO})$  bi-  
575 ases span (0.5–0.9)‰. Although not large, these well exceed the  $\delta^{13}\text{C}(\text{CO})$  measurement preci-  
576 sion of  $\pm 0.1\%$  and were corrected for, and therefore are taken into account in the calculations  
577 with the MM presented in Sect. 3.1.

Deleted: <sup>13</sup>C

Deleted: reckoned

Deleted: and

Deleted: 3

Deleted: (Assonov and Brenninkmeijer (2001))

## 578 Acknowledgements

579 [27] The authors are indebted to Claus Koepfel, Dieter Scharffe and Dr. Andreas Zahn for their  
580 work and expertise on the carbon monoxide and ozone measurements in C1 and C2. Hella  
581 Riede is acknowledged for comprehensive estimates of the species lifetimes along the  
582 CARIBIC flight routes. We are grateful to Dr. Taku Umezawa, Dr. Angela K. Baker, Dr. Em-  
583 ma C. Leedham, Dr. Sergey Assonov, the anonymous, reviewer and Dr. Jan Kaiser for the help-  
584 ful discussions and comments on the manuscript.

Deleted: and

Deleted: ACP

Deleted: s

## 585 References

- 586 Assonov, S. S. and Brenninkmeijer, C. A. M.: A new method to determine the  $^{17}\text{O}$  isotopic abundance in  
587 CO<sub>2</sub> using oxygen isotope exchange with a solid oxide, *Rapid Commun. Mass Spectrom.*, **15**,  
588 2426–2437, doi: [10.1002/rcm.529](https://doi.org/10.1002/rcm.529), 2001.
- 589 Assonov, S. S. and Brenninkmeijer, C. A. M.: A redetermination of absolute values for  $^{17}\text{R}_{\text{VPDB-CO}_2}$  and  
590  $^{17}\text{R}_{\text{VSMOW}}$ , *Rapid Commun. Mass Spectrom.*, **17**, 1017–1029, doi: [10.1002/Rcm.1011](https://doi.org/10.1002/Rcm.1011), 2003.
- 591 Assonov, S. S., Brenninkmeijer, C. A. M., Koepfel, C., and Röckmann, T.: CO<sub>2</sub> isotope analyses using  
592 large air samples collected on intercontinental flights by the CARIBIC Boeing 767,  
593 *Rapid Commun. Mass Spectrom.*, **23**, 822–830, doi: [10.1002/rcm.3946](https://doi.org/10.1002/rcm.3946), 2009.
- 594 Bhattacharya, S. K., Pandey, A., and Savarino, J.: Determination of intramolecular isotope distribution of  
595 ozone by oxidation reaction with silver metal, *J. Geophys. Res. Atm.*, **113**, D03303,  
596 doi: [10.1029/2006jd008309](https://doi.org/10.1029/2006jd008309), 2008.

## Tables

Table 1. Ozone  $^{18}\text{O}/^{16}\text{O}$  isotope ratios from literature and this study

Domain	T (K)	P (hPa)	$\delta^{18}\text{O}(\text{O}_3)$ (‰)	Remarks
Stratosphere	190–210	13–50	83–93 (<3)	1
UT/LMS	220–235	240–270	89–95 (8)	2
			84–88 (6)	T
			91–98 (9)	TC
			112–124 (17)	C
Laboratory	190–210	~67	87–97 (6)	3
	220–235	~67	102–110 (6)	3
	220–235	240–270	95–103	4

Notes: Values in parentheses denote the average of the estimates' standard errors. The expected  $\text{O}_3$  isotope composition on the V-SMOW scale is calculated from the  $\text{O}_3$  enrichments  $\epsilon$  reported relative to  $\text{O}_2$  using  $\delta^{18}\text{O}(\text{O}_3)_{\text{V-SMOW}} =$

$$\delta^{18}\text{O}(\text{O}_2)_{\text{V-SMOW}} + \frac{18}{2}\epsilon(\text{O}_2)_{\text{O}_2} + [\delta^{18}\text{O}(\text{O}_2)_{\text{V-SMOW}} \times \frac{18}{2}\epsilon(\text{O})_{\text{O}_2}]$$

<sup>1</sup> Observations (see Krankowsky *et al.* (2007) and refs. therein), lowermost values (19–25 km). Quoted temperature range is derived by matching measured  $\delta^{18}\text{O}(\text{O}_3)$  and laboratory data (see note <sup>3</sup>).

<sup>2</sup> This study, C1 observations (10–12 km). Letters denote the estimates derived using the data from Bhattacharya *et al.* (2008) and assuming only terminal (T), only central (C) and equiprobable terminal and central (TC)  $\text{O}_3$  atoms transfer to the artefact  $\text{CO}$ .

<sup>3</sup> Calculated using the laboratory KIE temperature dependence data summarised by Janssen *et al.* (2003).

<sup>4</sup> Calculated assuming a pressure dependence of the  $\text{O}_3$  formation KIE similar to that measured at 320 K (see Gunther *et al.* (1999) and refs. therein).

Deleted: [

Deleted: ]

Deleted: [

Deleted: ]

Deleted: [

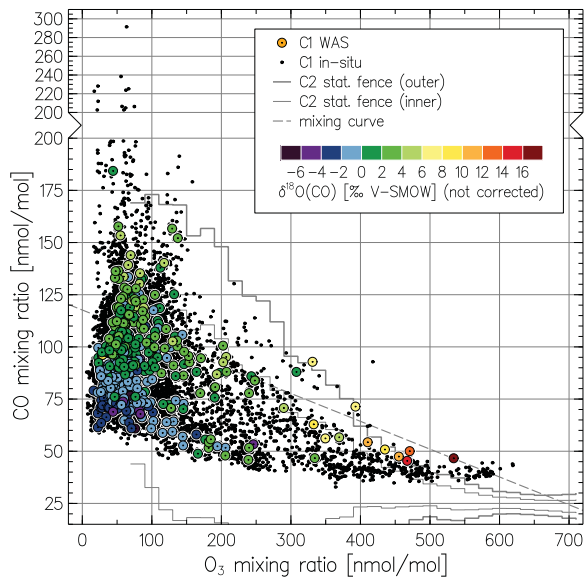
Deleted: ]

Deleted:  $^{18}\text{O}$

Deleted:  $^{18}\text{O}$

724 Fig. 1. (a) Distribution of CO mixing ratios as a function of concomitant O<sub>3</sub> mixing ratios measured by  
725 CARIBIC in the LMS ([O<sub>3</sub>]>300 nmol/mol). The shaded area is the two-dimensional histogram of the C2  
726 measurements (all C2 data obtained until June 2013) counted in 5×1 nmol/mol size [O<sub>3</sub>]×[CO] bins, thus  
727 darker areas emphasise greater numbers of particular CO–O<sub>3</sub> pairs observed. Small symbols denote the  
728 original C1 *in situ* measurements (black) and corrected for the artefacts (red); the C1 WAS analyses (11 of  
729 total 408) are shown with large symbols. Thin and thick step-lines demark the inner and outer statistical  
730 fences (ranges outside which the data points are considered mild or extreme outliers, see text) of the C2  
731 data, respectively. The dashed curve exemplifies compositions expected from the linear mixing of very  
732 different (*e.g.*, tropospheric and stratospheric) end-members. (b) Statistics on CO mixing ratios from C1  
733 and C2 data shown in box-and-whisker diagrams for samples clustered in 20 nmol/mol O<sub>3</sub> bins (whiskers  
734 represent 9<sup>th</sup>/91<sup>st</sup> percentiles). (c) Sample statistic for each CARIBIC dataset (note the C2 figures scaled  
735 down by a factor of 1000). (d) Estimates of the C1 *in situ* CO contamination strength  $C_c$  as a function of  
736 [O<sub>3</sub>] (solid line) obtained by fitting the difference  $\Delta\text{CO}$  between the C2 and C1 *in situ* [CO] (small sym-  
737 bols) in the kinetic framework (see Appendix A, Eq. (A1)). Step line shows the  $\Delta\text{CO}$  for the statistical av-  
738 erages (the shaded area equals the height of the inner statistical fences of the C2 data). Large symbols de-  
739 note the estimates of  $C_c$  in the C1 WAS data (slight variations vs. the *in situ* data are due to the sample  
740 mixing effects, see Sect. 3). Colour denotes the respective C1 WAS  $\delta^{18}\text{O}(\text{CO})$  (note that typically 6–7  
741 *in situ* measurements correspond to one WAS sample).

**Deleted:** Note: The entire C1 CO/O<sub>3</sub> dataset is presented in the Supplementary Material, Fig. S1.

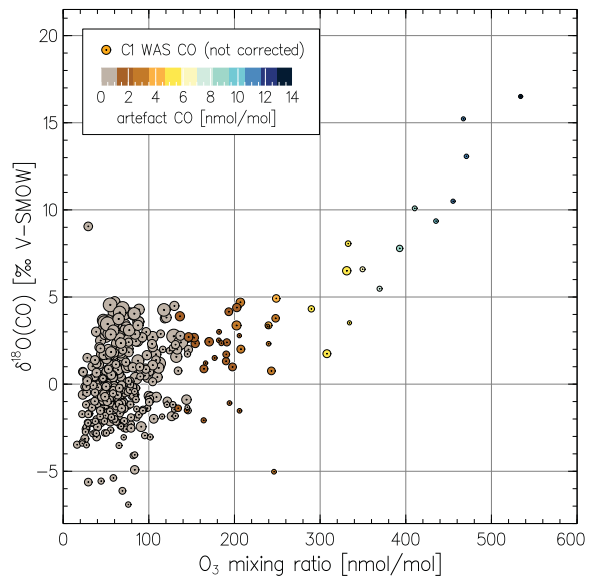


744 Fig. 2. (accompanies Fig. 1) Carbon monoxide and ozone mixing ratios measured in C1. Small black  
 745 symbols denote the C1 *in situ* measurements ( $n = 12753$ ). The C1 WAS analyses ( $n = 408$ ) are shown with  
 746 large symbols; colour denotes the concomitant  $\delta^{18}\text{O}(\text{CO})$  measurements. Thin and thick step-lines denote  
 747 the inner and outer statistical fences of the C2 data, respectively. The dashed curve exemplifies composi-  
 748 tions expected from the linear mixing of tropospheric and stratospheric end-members (see caption to Fig. 1  
 749 [for details](#)).

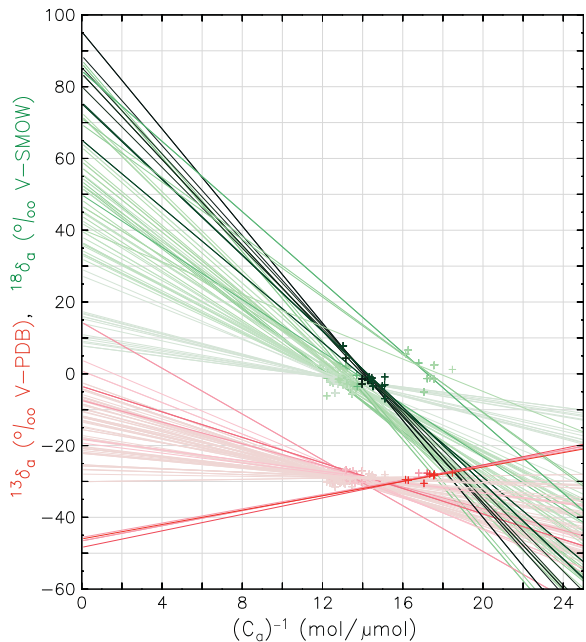
Deleted: (ranges outside which the data points are considered mild or extreme outliers)

Deleted: very different (e.g.,

Deleted: )



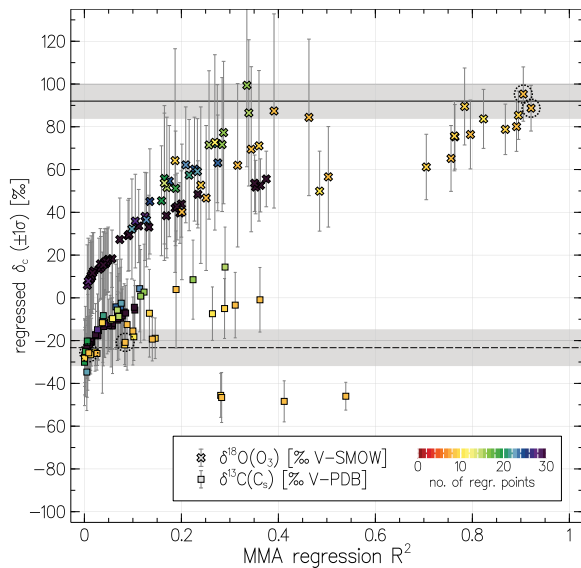
760 Fig. 4. Measured C1 WAS  $\delta^{18}\text{O}(\text{CO})$  (not corrected for artefacts) as a function of concomitant  $\text{O}_3$  mixing  
 761 ratio. Symbol colour denotes the artefact  $\text{CO}$  component (integral  $C_e$  per each WAS); symbol size scales  
 762 proportionally to the WAS  $\text{CO}$  mixing ratio corrected for artefacts (see Sect. 3 for details).



763 Fig. 5. Keeling plot of the data used in the calculations with the mixing model (MM). The CI WAS  
 764 isotope CO measurements are shown with symbols, solid lines denote the linear regressions through the vari-  
 765 ous sets of samples selected by the MM ( $n = 80$  sets are plotted). Colours refer to the  $\delta^{13}\text{C}$  (red) and  $\delta^{18}\text{O}$   
 766 (green) data, colour intensity indicates the coefficient of determination ( $R^2$ ) of each regression, respec-  
 767 tively. Darker colours denote higher  $R^2$  values, with maxima of 0.92 for  $\delta^{18}\text{O}$  and 0.54 for  $\delta^{13}\text{C}$  data, respec-  
 768 tively. The inferred contamination signatures ( $\hat{\phi}_c$ ) are found at  $(C_a)^{-1} \rightarrow 0$ . Regression uncertainties are  
 769 shown in Fig. 5. Note that because different subsets of samples contain same data points, some of the  
 770 symbols are plotted over (*i.e.*, not all symbols contributing to a particular regression case may be seen).

Deleted: /

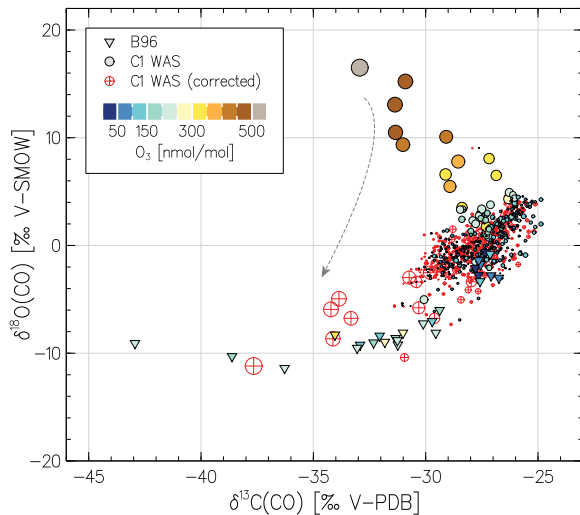




772 Fig. 6. Results of the regression calculation with the MM. Shown with symbols are the contamination  
 773 source isotope signatures  $\delta_c$  as a function of the respective coefficient of determination ( $R^2$ ). Colour  
 774 denotes the number of samples in each subset selected. Solid and dashed lines present the best guess  
 775  $\pm 1$  standard deviation of the mean for the  $\delta^{18}\text{O}(\text{O}_3)$  and  $\delta^{13}\text{C}(\text{C}_c)$  estimates. Dashed circles mark the values  
 776 obtained at highest  $R^2$  for  $^{18}\text{O}$  regression (above 0.9). See text for details.

Deleted: :

Deleted: SD



779 Fig. 7.  $^{18}\text{O}/^{16}\text{O}$  and  $^{13}\text{C}/^{12}\text{C}$  isotope composition of CO measured in C1. Triangles present the data from  
 780 the remote SH UT/LMS obtained by Brenninkmeijer *et al.* (1996) (B96). Colour refers to the concomitantly  
 781 observed  $\text{O}_3$  abundances; note the extremely low  $[\text{O}_3]$  encountered by B96 in the Antarctic ozone-hole  
 782 conditions. Filled and hollow circles denote the original and corrected (as exemplified by the dashed ar-  
 783 row) C1 WAS data, respectively, with the symbol size scaling proportional to the estimated contamination  
 784 magnitude (see [text](#) for details).

Deleted: the manuscript